Effects of Non-metallic Elements B, Si and Te on the Formation, Mechanical Properties and Microstructure of Cu-Zr-based Amorphous Alloys

Kaiyuan Xiao*

Department of Mechanical Engineering, Columbia University, New York, 10027, USA

*Corresponding author: kx2166@columbia.edu

Abstract. In recent years, the B2 CuZr crystals have been successfully introduced into the matrix of amorphous alloy, resulting in the formation of bulk metallic glass composite. The in situ fabricated amorphous composites have exhibited not only good plasticity but high yield strength in conjunction with obvious work-hardening behavior, which has attracted great attention. However, until now microalloying elements are mainly metallic elements and less studies have been conducted on the non-metallic elements on the glass-forming ability and mechanical properties of Cu-Zr-based metallic glasses and their composites. In this work, the influence of non-metallic elements B, Si and Te on the structural evolution and the mechanical properties in Cu-Zr-based metallic glass matrix composites were studied. It was found the that the prepared bulk metallic glass matrix composites show high strength and plasticity at room temperature. This work provides a good experimental basis for future application.

Keywords: amorphous alloys; bulk metallic glass matrix composite; microalloying; non-metallic elements; mechanical properties.

1. Introduction

The common structure of solid matter is generally crystalline, but there are also some non-crystalline structures. As can be seen from Figure 1, in the crystalline structure, the arrangement of atoms is periodic, with long-range order and translational symmetry, while the arrangement of atoms is long-range disorder in the amorphous structure. Amorphous substances formed in nature include glass (such as silicon dioxide), inorganic salts (such as calcium hydrogen phosphate), and some elementary substance (such as selenium), etc.

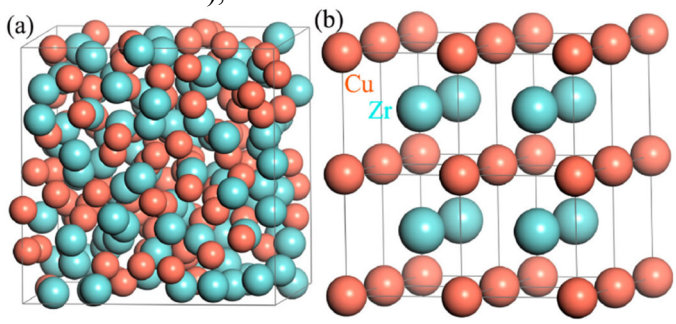

Fig. 1 Amorphous atomic structure and crystalline atomic structure in CuZr alloy [1]

Amorphous alloy or metallic glass refers to alloy with an amorphous structure. It is a new type of alloy material prepared by modern rapid cooling and solidification technology [2]. However, the difference from common glass is that in amorphous alloys, atoms are bonded to each other by metal bonds, so many properties related to metals are preserved. At the same time, its structure is similar to that of glass, which is an amorphous structure. During the general cooling process, the alloy will crystallize and the atoms will be arranged in an orderly manner according to certain rules. The alloy solidified through this process is a crystalline material (such as steel). By cooling the melt alloy rapidly, the atoms have no time to form an arranged crystalline structure. Therefore, the disordered state of atoms is preserved, which result in the formation of a thermodynamically incomplete structure with short-range order and long-range disorder-glass structure. Due to its unique disordered structure,

amorphous alloy exhibits exceptional properties such as corrosion resistance, high strength and hardness [3], which have attracted extensive attention from researchers and have become one of the hottest areas of research on metallic materials.

Cu-Zr-based amorphous alloys have great practical application value and development potential due to their high strength, good glass-forming ability (GFA), and relatively low manufacturing cost [4-6]. In previous studies, their focus was on the effect of the adding of metallic elements on the GFA and mechanical properties of the alloy system, and more meaningful data have been accumulated [7-9]. However, little was known about the influence of non-metallic elements on the properties of amorphous alloys, which inspired this paper. In summary, the main works of this experiment were

(1) Adjusted the composition of $(Cu_{50}Zr_{50})_{95}Al_5$ alloy, introducing non-metallic elements B, Si, Te. Prepared amorphous alloy with different alloy composition by rapid cooling method, and studied the effects of the addition of these three non-metallic elements on the GFA of alloy by X-ray Diffraction (XRD).

(2) Conducted compression experiments on the prepared amorphous alloy samples by mechanical testing machine to obtain their room temperature mechanical property parameters. Analyzed the microstructure and morphology of their compression fractures through Scanning Electron Microscope (SEM) to find information on their structural evolution during room temperature plastic deformation.

2. Experimental procedures

(1) Preparation for alloy ingots:

Prepared simple substances needed according to the atomic ratio: $(Cu_{50}Zr_{50})_{95}Al_5$, $(Cu_{50}Zr_{50})_{95-X}Al_5B_X$ (X=0.5, 1, 1.5), $(Cu_{50}Zr_{50})_{95-X}Al_5Si_X$ (X=0.5, 1, 1.5), $(Cu_{50}Zr_{50})_{95-X}Al_5Te_X$ (X=0.5, 1, 1.5). The purity of all raw materials used were 99.99%.

The simple substances were melted using a vacuum arc melting furnace under argon gas protection, and the alloy ingots were repeatedly melted several times to keep them homogeneous.

(2) Preparation for amorphous alloys:

This experiment required amorphous alloy bar samples, which were fabricated by the suction-casting methods.

(3) Testing of the experimental samples:

XRD tests and axial compression tests were performed on the bar samples, and their microstructure and morphology of the fractures were observed by SEM.

3. Experimental results and discussion

3.1 Effect of the addition of non-metallic elements B, Si, and Te on the GFA of Cu-Zr-based amorphous alloys

Figure 2 shows the XRD pattern corresponding to the bar samples with B element added. From the figure, it can be seen that when no B element is added, the diffraction curve is diffuse, indicating that the alloy is almost pure amorphous structure. After the addition of element B, several obvious crystalline peaks appear on the diffraction pattern, and their corresponding phases are B2 CuZr, CuZr martensite and $Cu_{10}Zr_7$. The XRD pattern suggests that the adding of B reduces the GFA of the alloy bar.

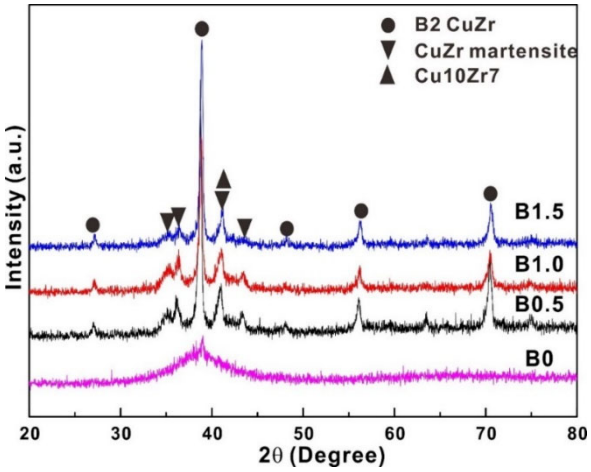

Fig. 2 XRD pattern for B-added bar

As can be seen from Figure 3, when the Si content is 0 and 0.5%, the diffraction pattern is diffuse in the whole 2θ range, indicating that these two samples are almost pure amorphous structures. When the Si content increased to 1.0% and 1.5%, obvious crystal peaks appeared, and the corresponding phases are found to be B2 CuZr, CuZr martensite and $Cu_{10}Zr_7$.

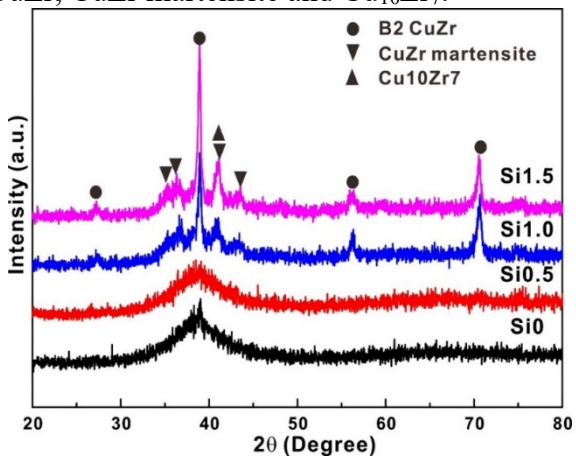

Fig. 3 XRD pattern for Si-added bar

In Figure 4, a B2 CuZr crystal peak appears when the Te content is 1.5%. The XRD pattern doesn't show apparent crystal peak when the content of Te is less than 1.5%.

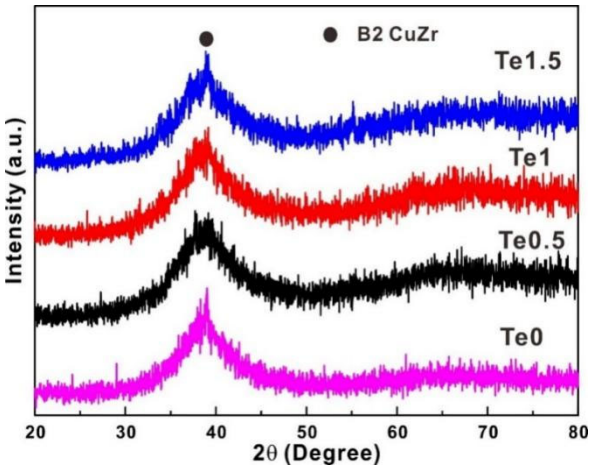

Fig. 4 XRD pattern for Te-added bar

3.2 Effect of the addition of non-metallic elements B, Si, and Te on the mechanical properties and fracture morphology of Cu-Zr-based amorphous alloys

Figure 5 and Table 1 show that $Cu_{47.5}Zr_{47.5}Al_5$ has high strength, but its room temperature plastic strain is small.

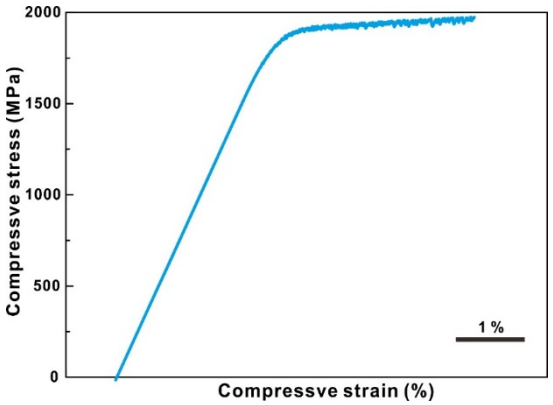

Fig. 5 Axial compressive stress-strain curve of $Cu_{47.5}Zr_{47.5}Al_5$ bar

Table 1. Mechanical properties for $Cu_{47.5}Zr_{47.5}Al_5$ bar

Compositions	Yield strength	Fracture strength	Plastic strain
Al5	1871 ± 20 MPa	1967 ± 20 MPa	2.8 ± 0.5 %

Figure 6 and Table 2 show that the yield strength of the alloy decreases after the adding of B. This is because the crystalline phases cannot play a good role in strengthening the matrix, but the appearance of these crystalline phases significantly improves the plasticity of the alloy bars.

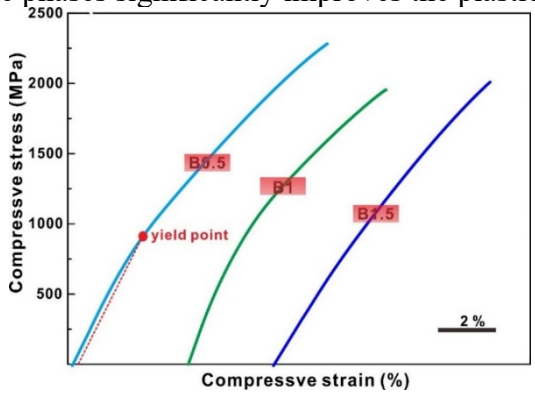

Fig. 6 Axial compressive stress-strain curve of B-added bar

Table 2. Mechanical properties for B-added bar

Compositions	Yield strength	Fracture strength	Plastic strain
B0.5	903 ± 70 MPa	2281 ± 70 MPa	6.4 ± 0.5 %
B1	835 ± 80 MPa	1955 ± 70 MPa	5.1 ± 0.5%
B1.5	830 ± 50 MPa	2010 ± 70 MPa	4.8 ± 0.5%

From Figure 7, when the Si content is 0.5% and 1%, the shape of the compression curve shows that the bar undergoes significant brittle fracture. However, when the Si content continues to increase to 1.5%, the shape of the curve is completely different from the previous curves. It no longer shows brittle fracture, but has greater plasticity despite some decrease in yield strength. According to the previous analysis, the Si1.5 bar has more B2 CuZr crystalline phase whose presence could improve the room temperature plasticity of the alloy bar. Table 3 shows the mechanical properties of the silicon added bar.

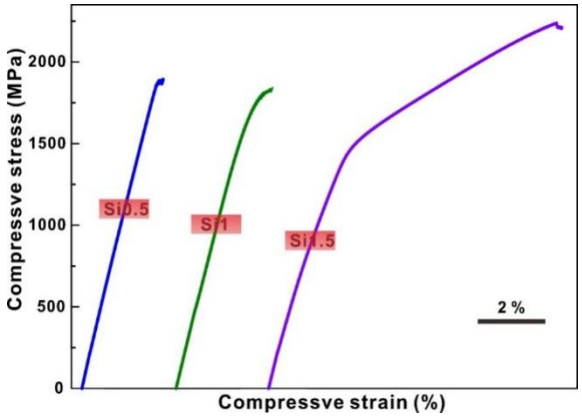

Fig. 7 Axial compressive stress-strain curve of Si-added bar

Table 3. Mechanical properties for Si-added bar

Compositions	Yield strength	Fracture strength	Plastic strain
Si1.5	1436 ± 10 MPa	2210 ± 50 MPa	6.4 ± 0.5 %

Figure 8 is the image for SEM observation. (a) is the surface image of the Si1.5 bar after fracture. (b) is an enlarged image of a specific area of (a), and (c) is a further enlarged view of (b). (d) is the enlarged view of the fracture corresponding to Si1.0. (e) is the enlarged image of the fracture corresponding to B0.5.

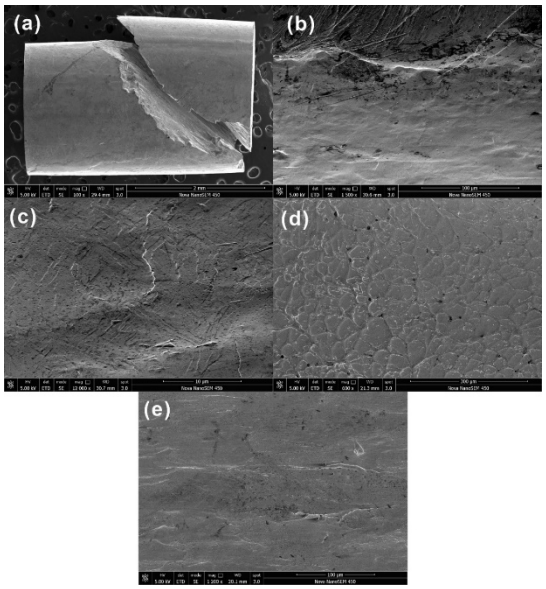

Fig. 8 Image for SEM observation

No obvious shear band is observed in (a). In (b), a clear boundary between crystal and amorphous structure exists. Above the boundary is the amorphous structure and shear bands can be seen, and the lower part is the crystalline structure without the existence of shear bands. The presence of martensite is also found, which corresponds to the XRD pattern. (d) is a characteristic SEM image of the fracture surface from an amorphous alloy, where the vein-like texture after the deformation can be clearly observed. (e) is a texture of crystal after deformation, indicating that there are crystals in B0.5 bar.

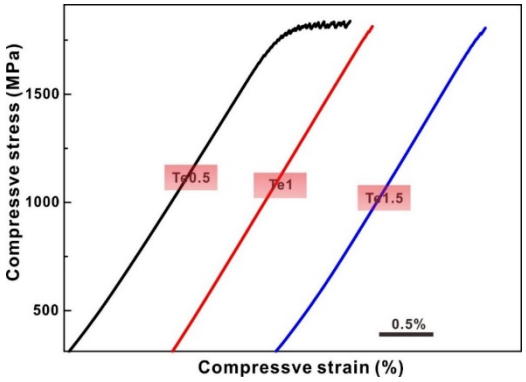

Fig. 9 Axial compressive stress-strain curve of Te-added bar

Table 4. Mechanical properties for Te-added bar

Compositions	Yield strength	Fracture strength	Plastic strain
Te0.5	1808 ± 20 MPa	1825 ± 50 MPa	0.5 ± 0.2 %

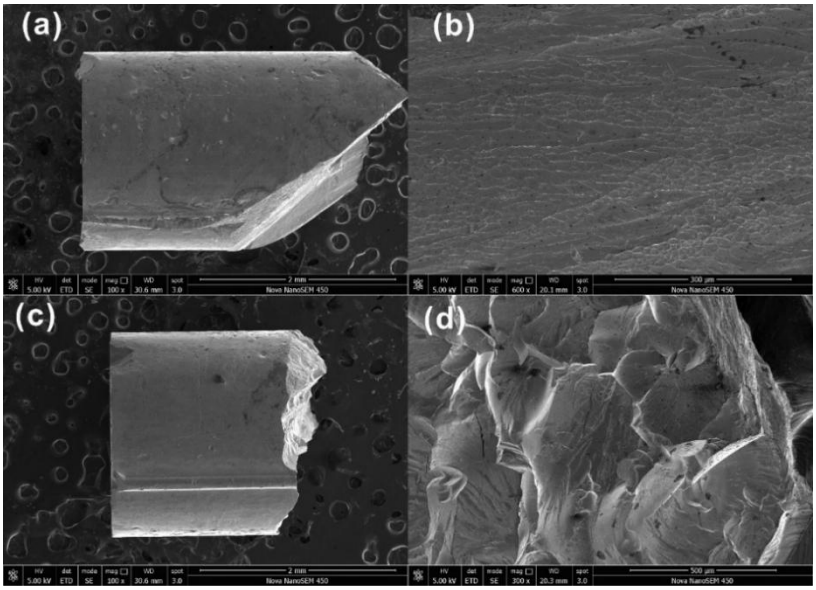

Fig. 10 Image for SEM observation

In Figure 9 and Table 4, it can be noticed that the yield strength and fracture strength of the alloy with Te content of 0.5% are lower than those of $Cu_{47.5}Zr_{47.5}Al_5$, and the plasticity is not as good as that of $Cu_{47.5}Zr_{47.5}Al_5$. The fracture pattern exhibited by the curve also becomes brittle fracture as the content of Te increases to 1% and 1.5%. Figure 10 shows the SEM observation. (a), (b) correspond to Te0.5, and (c), (d) correspond to the Te1.5. It can be noticed in (a) that the fracture mode of Te0.5 is still shear fracture. (b) shows the vein-like texture which is a characteristic of amorphous alloy after deformation. (c) suggests that the fracture mode of Te1.5 is no longer shear fracture but a direct fracture at about 90 degrees, indicating that the adding of Te element also affects the fracture form of the alloy.

4. Conclusion

(1) XRD tests were carried out on the alloy rods to obtain their diffraction pattern. It was observed that the adding of B element weakened the GFA of the alloy. The addition of a small amount of Si has little effect on the amorphous forming ability, but too much will reduce the amorphous forming ability. The effect of crystal forming ability is similar to that of Si.

(2) The alloy rods were subjected to axial compression test, and the fracture was observed by SEM. It was found that the addition of B decreased the yield strength of the alloy, but improved the plasticity.

The addition of Si element enhanced the plasticity of the amorphous alloy at room temperature. The fracture mode was changed by adding Te, and its mechanical properties could not be improved.

(3) The following reasonable inference can be drawn from the above analysis, the addition of non-metallic elements B, Si and Te can alter the GFA and mechanical properties of alloy of Cu-Zr-Al alloy system. By appropriately adjusting the content of non-metallic elements, the plasticity of the alloy can be enhanced while retaining its strength to the greatest extent.

References

[1] Qiao J., Jia H., Liaw P. K. Metallic glass matrix composites. Materials Science & Engineering R Reports, 2016, 100(2): 1-69.

[2] W., H. , Wang, C., Dong, C., H. , & Shek. (2004). Bulk metallic glasses. Materials Science & Engineering R Reports.

[3] Telford M. The case for bulk metallic glass. Materials Today, 2004, 7(3): 36-43.

[4] Zhang W., Zhang Q., Inoue A. Synthesis and mechanical properties of new Cu-Zr-based glassy alloys with high glass-forming ability. Advanced Engineering Materials, 2010, 10(11): 1034-1038.

[5] Janovszky D., Tranta F., Solyom J., Roosz A. Glass forming ability of bulk amorphous materials in Cu-Zr-Ag ternary alloy systems. Materials Science Forum, 2013, 729: 373-378.

[6] Zhang Q. S., Zhang H. F., Deng Y. F., Ding B. Z., Hu, Z. Q. Bulk metallic glass formation of Cu-Zr-Ti-Sn alloys. Scripta Materialia, 2003, 49(4): 273-278.

[7] J., Chen, and, Y., Zhang, & and, et al. (2006). Metallographic analysis of Cu–Zr–Al bulk amorphous alloys with yttrium addition. Scripta Materialia.

[8] Wang Y., Li L., Sun C., Lu Q. Rare earth elements on glass-forming ability and thermal stability of Cu-Zr-Al metallic glass. Materials Science Forum, 2011, 688: 426-430.

[9] Fu J., Hua M., Pang S., Ma C., Tao Z. Formation and thermal stability of Cu-Zr-Al-Er bulk metallic glasses with high glass-forming ability. Journal of University of Science & Technology Beijing, 2007, 14: 36-38.